Synthesis and Spectroscopic Characterization of Zinc Tetra(3,4-pyridine)Porphyrazine Entrapped within the Supercages of Y-Zeolite

Witold S. Szulbinski and James R. Kincaid*

Department of Chemistry, Marquette University, Milwaukee, Wisconsin 53201-1881

Received August 29, 1997

In this work, the generation of Y-zeolite-entrapped zinc tetra(3,4-pyridine)porphyrazine (ZnPz-Z) at several loading levels is reported. The ZnPz-Z samples were obtained using the template synthesis method involving condensation of 3,4-dicyanopyridine (DCP) around Zn^{2+} cations which had been ion-exchanged into the Y-zeolite supercages (Zn^{2+}-Z). The integrity of the sample was documented by diffuse reflectance (DR), emission (Em) and resonance Raman (RR) spectroscopic data. The Raman spectrum for the ground-state ZnPz-Z intrazeolitic complex, with the laser excitation at $\lambda_{ex} = 568.2$ nm, closely matched that obtained for the free ZnPz porphyrazine, with some bands exhibiting slight frequency shifts of $1-5$ cm^{-1}. The DR spectrum of ZnPz-Z exhibited maxima at $\lambda_{max} =$ 414 and 682 nm, and the emission spectrum of ZnPz-Z revealed fluorescence at $\lambda_{em} = 705$ nm, with $\lambda_{ex} = 350.9$, 406.7, or 647.1 nm. This emission was 22 nm red shifted with respect to that recorded for the free ZnPz complex in pyridine solution and 24 nm red shifted relative to that acquired for the ZnPz complex adsorbed on the outer surface of the zeolite. All these spectroscopic data suggest that the ZnPz molecules within the zeolite supercages were only slightly distorted. The ZnPz-Z samples contain a small amount of luminescent ($\lambda_{em} = 500$ nm) impurities assigned to products of 3,4-dicyanopyridine noncyclic condensation.

Introduction

For the past fifteen years, there has been much interest in the development of catalytic systems based on intrazeolitic metal complexes.[1−7] It has been shown that the zeolite framework effectively prevents certain catalysts from undergoing degradation reactions which, in free solution, arise from photoinduced deligation,[5a,b] dimerization, or autoxidation.[7a] For example, such zeolite-entrapped species are more efficient reversible oxygen carriers than the homogeneous solution complexes which readily degrade.[2b,3] Also, in the area of photocatalyzed electron-transfer schemes, the guest/host interactions significantly retard the energy wasting back-electron-transfer reaction of initial photoproducts.[4−6] Moreover, it has been demonstrated that the intrazeolitic complexes which possess ligands bearing a peripheral nitrogen atom, such as Z-Ru(bpy)$_2$(bpz)$^{2+}$ (where bpz is 2,2′-bipyrazine), are susceptible to coordination of another molecule of Ru^{2+} complex.[5c,d] This approach is expected to provide highly efficient photocatalysts for solar energy conversion owing to the unique reactivity and spatial distribution of the appropriate components.[4c,5c]

Up to now, three methods for generation of intrazeolite metal complexes have been developed. These are the flexible ligand method,[7] the template ("ship in the bottle") synthesis,[2] and the crystallization inclusion (zeolite synthesis) method.[8] Based on molecular graphics analysis, it has been argued that in the case of Y-zeolite-encapsulated phthalocyanines (Pc), the planarity of the complex must be disturbed, since the dimensions of the ligand (i.d. 14−15 Å) exceed the effective diameter of the zeolite supercages (∼ 13 Å).[7a] Herron[2c] proposed that molecules of intrazeolitic FePc have a saddle-shaped structure with the benzene groups protruding out of the 7 Å windows of the supercages. This should result in the FePc symmetry being lowered from D_{4h} to D_{2d}.[2c] Clearly, phthalocyanines and porphyrazines cannot be incorporated directly into the ∼13 Å Y-zeolite supercages by the first method because they cannot pass through the 7 Å windows. Thus, the most promising method for the generation of intrazeolitic metallophthalocyanines would seem to be the template synthesis. However, Wöhrle and co-workers[8] recently reported the successful incorporation

(1) DeWilde, W.; Peeters, G.; Lunsford, J. H. *J. Phys. Chem.* **1980**, *84*, 2306−2310.
(2) (a) Herron, N. *Inorg. Chem.* **1986**, *25*, 4714. (b) Herron, N.; Stucky, G. D.; Tolman, C. A. *J. Chem. Soc., Chem. Commun.* **1986**, 1521−1522. (c) Herron, N. *J. Coord. Chem.* **1988**, *19*, 25−38. (d) *Inclusion Chemistry with Zeolites*; Herron, N., Corbin, D. R., Eds.; Kluwer: Dordrecht, 1995 and refrences therein.
(3) (a) Nakamura, M.; Tatsumi, T.; Tominaga, H. *Bull. Chem. Soc. Jpn.* **1990**, *63*, 3332−3336. (b) Zhan, B.-Z.; Li, X.-Y. *J. Chem. Soc., Chem. Commun.* **1998**, 349−350.
(4) (a) Borja, M.; Dutta, P. K. *Nature* **1993**, *362*, 43−45. (b) Ledney, M.; Dutta, P. K. *J. Am. Chem. Soc.* **1995**, *117*, 7687−7695. (c) Dutta, P. K.; Ledney, M. *Progress in Inorganic Chemistry*; J. Wiley & Sons: New York, 1997; Vol. 44, p 209−271.
(5) (a) Maruszewski, K.; Strommen, D. P.; Kincaid, J. R. *J. Am. Chem. Soc.* **1993**, *115*, 8345−8350. (b) Maruszewski, K.; Kincaid, J. R. *Inorg. Chem.* **1995**, *34*, 2002. (c) Sykora, M.; Maruszewski, K.; Treffert-Ziemelis, S. M.; Kincaid, J. R. *J. Am. Chem. Soc.* **1998**, *120*, 3490−3498. (d) Sykora, M.; Kincaid, J. R. *Nature* **1997**, *387*, 162−164.
(6) (a) Kalyanasundaram, K. *Photochemistry in Microheterogenous Systems*; Academic Press: Orlando, FL, 1987. (b) Ramamurthy, V.; *Photochemistry in Organized and Constrained Media*; VCH: New York, 1991.
(7) (a) Bedioui, F. *Coord. Chem. Rev.* **1995**, *144*, 39−68. (b) Carrado, K. A.; Thiyagarajan, P.; Winans, R. E.; Botto, R. E. *Inorg. Chem.* **1991**, *30*, 794−799. (c) Ferraris, J. P., Balkus, K. J., Jr.; Schade, A. *J. Incl. Phenom. Mol. Recog. Chem.* **1992**, *14*, 163−169. (d) Balkus, K. J., Jr.; Gabrielov, A. G.; Bell, S. L.; Bedioui, F.; Roue, L.; Devynck, J. *Inorg. Chem.* **1994**, *33*, 67−72. (e) Paez-Mozo, E.; Gabriunas, N.; Lucaccioni, F.; Acosta, D. D.; Patrono, P.; La Ginestra, A.; Ruiz, P.; Delmon, B. *J. Phys. Chem.* **1993**, *97*, 12819−12827. (f) Balkus, K. J., Jr.; Eissa, M.; Levado, R. *J. Am. Chem. Soc.* **1995**, *117*, 10753−10754.
(8) (a) Wöhrle, D.; Sobbi, A. K.; Franke, O.; Schulz-Ekloff, G. *Zeolites* **1995**, *15*, 540−550. (b) Hoppe, R.; Schulz-Ekloff, G.; Rathousky, J.; Starek, J.; Zukal, A. *Zeolites* **1994**, *14*, 126. (c) Wohlrab, S.; Hoppe, R.; Schulz-Ekloff, G.; Wöhrle, D. *Zeolites* **1992**, *12*, 862.

S0020-1669(97)01118-X CCC: $15.00
Published on Web 09/03/1998

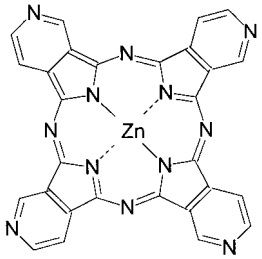

ZnPz

Figure 1. Schematic representation of ZnPz.

of selected Zn^{2+} metalloporphyrins and metalloporphyrazines into molecular sieves using the crystallization inclusion method.

Herein are reported our efforts to generate the intrazeolitic Zn^{2+} tetra(3,4-pyridine)porphyrazine (ZnPz-Z) by the template synthesis method (for a schematic representation of the ZnPz complex see Figure 1). This approach offers an important advantage over the crystallization inclusion method for such large macrocycles. Thus, as has been pointed out by Wöhrle et al.,[8] the great tendency of some metal complexes, such as porphyrins and phthalocyanines, aggregation may lead to the inclusion of dimers or larger clusters[8a] which obviously could prohibit formation of Y-zeolite supercages in the vicinity of the clusters. In contrast, the template synthesis approach should facilitate synthesis of monomeric complexes isolated in individual supercages. While the material produced here contains a small amount of luminescent impurities (presumably, coming from products of partial condensation of DCP), the spectroscopic properties of the major component are consistent with those expected for the target complex.

Experimental Section

Materials and Synthesis. Tetra(3,4-pyridino)porphyrazine (Pz) and zinc tetra(3,4- pyridino)porphyrazine (ZnPz) were synthesized utilizing the method developed by Brach et al.[10] i.e., the condensation of 3,4-dicyanopyridine in *N*,*N*-dimethylaminoethanol bubbled with ammonia, at 130 °C. For the synthesis of ZnPz the stoichiometric amount of zinc acetate was used. The structure and purity of the metal-free Pz porphyrazine and the ZnPz complex was confirmed by UV−visible, ^{1}H NMR, mass spectroscopy, and elemental analysis. The latter indicated that the ZnPz sample was slightly contaminated. With reference to the synthesis of phthalocyanine analogues,[11] the ZnPz complex might be contaminated with products of noncyclic oligomers of 3,4-dicyanopyridine and their derivatives. For example, phthalocyanines prepared from 1,2-dicyanobenzene (DCB) contain around 0.1% impurities coming from products of partial (noncyclic) condensation of DCB.

Elemental Analysis. Calculated for $C_{28}H_{12}N_{12}Zn\cdot H_2O$: H, 2.35; C, 56.06; N, 28.02. Found: H, 2.64; C, 56.53; N, 28.99.

The FAB mass spectrum in the 3-NBA matrix displayed the expected molecular ion peak for $ZnPz^+$ at *m*/*z* 581.

Preparation of Intrazeolitic Zn^{2+} Tetra-3,4-pyridinoporphyrazine (ZnPz-Z). The Y-zeolite samples were purchased from Aldrich Chemical Co. (Milwaukee, WI). Typically, 2.0 g of the zeolite (calcinated at 500 °C, and then washed with 10% aqueous NaCl)[4c] was ion exchanged with appropriate amounts of $Zn(CH_3COO)_2\cdot 2H_2O$ in 300 mL of deionized (DI) water at pH = 5.4 (the pH was adjusted with 0.1 N HCl), so as to obtain five Zn^{2+}-exchanged (Zn^{2+}-Z) samples with the following loads: (1:15), (1:10), (1:5), (1:2), and (1:30); i.e., one Zn^{2+} cation per *x* supercages. The load of the resulting Zn^{2+}-Z samples was estimated assuming that 2 g of the zeolite-Y contained 5.556×10^{20} supercages. [9] During the ion-exchange operation, the solution was stirred vigorously at 4 °C, for 24 h. The zeolite was then filtered, washed with DI water, and air-dried. After that, the Zn^{2+}-Z zeolite was placed in a vacuum tube with a volume of 25 cm^3 and activated at 100−110 °C under a vacuum of 10^{-3} Torr for 5 h, and then an appropriate amount of 3,4-dicyanopyridine (DCP) was added. For details regarding the reagent ratios see Table 1. The solid mixture was again evacuated to 10^{-3} Torr and held at that pressure for the next 6 h. Subsequently, the vessel's stopcock was closed and the powder was heated at 200−210 °C for 3 days, during which time the sample changed color to blue (if the zeolite was not preactivated at 100−110 °C it changed to green, vide infra). After cooling, the crude product was washed with 20% aqueous NaCl (3×100 mL), and then with 500 mL of DI water. After drying under a stream of air, the zeolite was extracted with pyridine, in a Soxhlet apparatus, for 4−6 weeks until the free Pz porphyrazine and ZnPz were not detected in the extract, as documented by UV−visible and emission spectroscopy measurements. Subsequently, the zeolite was Soxhlet extracted with acetone and ethanol for 7 days each, until the extracts did not show the absorption of pyridine at 280 nm. Finally, the Z-ZnPz zeolite was stirred in 200 mL of boiling 20% aqueous NaCl (3 times for 3 days each), then filtered, washed with DI water (3×500 mL), and dried under a stream of nitrogen at 110 °C.

Table 1. Effect of Zn^{2+}-Z and DCP-Z Loads on the Generation of ZnPz-Z, Where I_{500}:I_{705} Is the Ratio of Luminescence Acquired for Purified ZnPz-Z Samples at 705 and 500 nm, $\lambda_{ex} = 351$ nm, 23 °C

Zn^{2+}-Z (Zn^{2+}/SC)[a]	reagents ratio 4DCP/Zn^{2+}-Z	DCP-Z (DCP/SC)[b]	ZnPz-Z generation	emission ratio I_{500}:I_{705}
1:2	1:1	2:1	no	1:0
	5:1	10:1	yes	10:1
1:5	1:1	0.8:1	no	1:0
	5:1	4:1	yes	22:1
	10:1	8:1	yes	20:1
1:10	5:1	2:1	no	1:0
	10:1	4:1	yes	1:3
1:15	5:1	1.3:1	no	1:0
	10:1	2.7:1	yes	1:3
1:30	5:1	0.7:1	no	1:0
	10:1	1.3:1	no	1:0
	25:1	3.3:1	no	1:0

[a] Zn^{2+} ion per number of supercages. [b] Number of DCP molecules per one supercage.

Preparation of ZnPz Complex Adsorbed onto the Outer Surface of the Y-Zeolite (Z/ZnPz). The Z/ZnPz sample was obtained by stirring of 2.0 g of the calcinated zeolite in 250 mL of freshly distilled pyridine, containing 10^{-5} M of the ZnPz complex (for 24 h at room temperature, in the dark). The zeolite sample was then filtered and dried under air.

Preparation of NH_4^+-Exchanged Y-Zeolite (NH_4^+-Z). The NH_4^+-Z sample was obtained by stirring of 2 g of calcinated Y-zeolite with aqueous 0.1 M NH_4Cl (500 mL) for 24 h, at 23 °C.[9]

Spectroscopic Measurements. UV−visible absorption spectra were obtained with a Hewlett-Packard model 8452A diode array spectrometer. To obtain the electronic spectra of intrazeolitic ZnPz, the zeolite framework (20−30 mg) was destroyed by treating with 3% HF (4 mL), and, after pH adjustment to 4 (with 0.1 N NaOH), the resulting solution was centrifuged (8000 rpm, for 0.5 h, 4 °C).

Resonance Raman (RR) spectra were acquired using a Spex 1269 spectrometer equipped with a Princeton Instruments ICCD-576 UV-enhanced detector and 356, 413, or 532 nm notch filters (Kaiser Optical Systems, Ann Arbor, MI), or a conventional Raman spectrometer (Spex model 1403 double monochromator equipped with a Spex model DM1B controller and a Hamamatsu R928 PMT). Excitation lines at 350.9, 406.7, 568.2, and 647.1 nm were from a Coherent model Innova 100-K3 Kr^+ ion laser. Spectra of the Pz, ZnPz, and ZnPz-Z complexes

(9) Breck, D. W. In *Zeolite Molecular Sieves*; John Wiley & Sons: New York, 1974.
(10) Brach, P. J.; Grammatica, S. J.; Ossana, O. A.; Weinberger, L. *J. Heterocycl. Chem.* **1970**, *7*, 1403−1405.
(11) (a) Moser, F. H.; Thomas, A. L. *Phthalocyanine Compounds*; Reinhold Publishing Corporation: New York, 1963. (b) Frraudi, G. In *Phthalocyanines Properties and Applications*; Leznoff, C. C., Lever, A. B. P., Eds.; VCH Publishers Inc.: New York, 1989; p 297−339. (d) *Macrocyclic Chemistry*; Dietrich, B., Viout, P., Lehn, J.-M., Eds.; VCH: New York, 1993.

diluted in solid KBr were obtained in rotating NMR tubes (5 i.d.) to avoid localized heating by the laser beam. The scattered light was collected with 135° back-scattering geometry and a conventional two-lens collection system. Before the measurements, the samples were degassed (at 10^{-4} Torr for 3 h) directly in the NMR tubes and then sealed. The spectroscopic apparatus used to acquire the emission spectra was the same as for the Raman measurements (Spex model 1403). The laser excitation was focused onto spun NMR tubes containing solid samples with the laser power of 10−20 mW at the sample. Spectra were recorded with 20−40 cm^{-1} increments.

Diffuse reflectance (DR) spectra were obtained with a Perkin-Elmer 320 spectrometer equipped with a Hitachi integrating sphere attachment. The samples were prepared as KBr pellets (typically 0.5−1 mg of Pz, ZnPz, or ZnPz-Z was mixed with 2 g of KBr) and a pellet with identical content of Na^+-Z zeolite was used as a blank. Finely ground $BaSO_4$ was applied as a reference. The spectra recorded in the transmittance mode were numerically converted using the Kubelka−Munk equation[12] with Spectracalc software.

^{1}H NMR spectra were acquired using a GE QE 300 MHz spectrometer. All spectra were obtained in deuterated solvents (CF_3-COOD or pyridine-d_5).

Mass spectra were obtained using a VG ZAB HS mass spectrometer (at the Nebraska Center for Mass Spectrometry, Lincoln, NE) equipped with a xenon gun. Several matrixes were used, including 3-NBA (3-nitrobenzyl alcohol).

Gas chromatography−mass (GC−MS) spectra were acquired with a 5890A gas chromatograph (Hewlett-Packard) equipped with a 5970 Series mass selective detector and a 59822A gauge controller (Hewlett-Packard). The injected samples were prepared in ethyl acetate or methylene chloride solutions.

Results and Discussion

Synthesis, Purification, and Analysis of ZnPz-Z. It has been well documented[2,7] that the condensation of 1,2-dicyanobenzene around appropriately cation-exchanged Y-zeolite leads to the generation of intrazeolitic metallophthalocyanines. Thus, to obtain the zeolite-entrapped ZnPz porphyrazine within the supercages (ZnPz-Z), a finely ground mixture of Zn^{2+}-Z and 3,4-dicyanopyridine (DCP) was heated at 200−210 °C, under a vacuum of 10^{-3} Torr. The loads of Zn^{2+}-Z (Zn^{2+} ion per number of supercages, Zn^{2+}/SC) and DCP-Z (number of DCP molecules per supercage, DCP/SC), as well as the ratio of the DCP/Zn^{2+}-Z reagents applied to the reaction, are listed in Table 1.

For every level of the Zn^{2+}-Z load a minimal amount of DCP was required, below which the DCP cyclization to ZnPz-Z did not occur; however, the generation of other products, apparently DCP noncyclic oligomers and their derivatives, was observed (vide infra). As evidenced by emission spectroscopy (see Table 1) for the lower Zn^{2+}-Z loads a larger excess of DCP was required. For example, for the load of 1:2 (one Zn^{2+} per 2 supercages), a 5-fold excess of DCP (with respect to the stoichiometric amount) was sufficient to complete the formation. On the other hand, for the load of 1:30 (one Zn^{2+} per 30 supercages) even a 25-fold excess of the DCP was too small to generate the ZnPz-Z complex. This observation can be explained in terms of the DCP-Z loading level, i.e., the generation of ZnPz-Z occurs efficiently if every supercage is occupied by at least 4 molecules of DCP (production of ZnPz molecule requires 4 DCP), as documented in Table 1.

We note that it appears to be important to reduce the level of moisture within the Zn^{2+}-loaded zeolite prior to the condensation reaction. Thus, samples should be heated at 100−110 °C for 5 h (at ~10^{-3} Torr). Samples which were not heated during the evacuation step resulted in a green product, the HF extract exhibiting extra bands at λ_{max} = 350 and 262 nm. On the basis of the proposed mechanism of formation of related phthalocyanines,[10,11] such impurities (yellow in color) probably arise by reaction of transient intermediate radicals ([DCP]$^{\bullet}_2$ and [DCP]$^{\bullet}_3$) with water and oxygen.

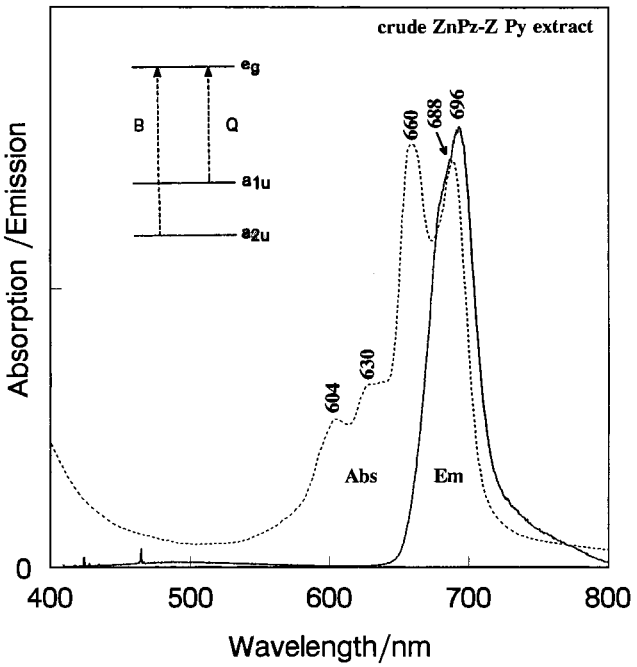

Figure 2. UV−visible and emission (λ_{ex} = 406.7 nm, 23 °C) spectra of ZnPz-Z (1:15) pyridine extract obtained after 2 weeks of extraction. The insert shows a diagram of the porphyrazine HOMO−LUMO orbitals.[11b]

To remove the excess of 3,4-dicyanopyridine from the crude ZnPz-Z product, the sample was extracted with pyridine in a Soxhlet apparatus. However, for ZnPz-Z with loads of 1:5; 1:10, and 1:15, the UV−visible spectrum of this extract (Figure 2, dotted line) showed absorption bands at wavelengths typical of the metal-free porphyrazine, and its emission spectrum acquired after 2 weeks of extraction exhibited luminescence centered at λ_{em} = 696 nm (Figure 2, solid line). This band appears as a superposition of two emissions centered at λ_{em} = 683 and 696 nm, which closely match those of the ZnPz complex[13] and the free Pz porphyrazine[11b] respectively. The Pz and ZnPz macrocycles contained in this extract were apparently adsorbed onto the outer surface of the zeolite, since they were effectively washed out using pyridine as the eluent (they are too large to diffuse out of the supercages). This observation indicates that a part of the DCP reagent, which did not associate with the intrazeolitic Zn^{2+} cations, was transformed into extrazeolitic Pz and ZnPz. The formation of the latter complex apparently involved those Zn^{2+} cations which were localized on the outer surface of the zeolite. On the other hand, for Zn^{2+}-Z with the load of 1:30, production of only noncyclic DCP oligomers was observed, as documented by emission spectroscopy. This finding indicates that noncyclic DCP condensation dominates if the concentration of intrazeolitic Zn^{2+}

(12) Frei, R. W.; MacNeil, J. D. *Diffuse Reflectance Spectroscopy in Environmental Problem-Solving*; CRC Press: Cleveland, OH, 1973; p 3−19.

(13) (a) Wöhrle, D.; Gitzel, J.; Okura, I.; Aono, S. *J. Chem. Soc., Perkin Trans. 2* **1985**, 1171−1178. (b) Richoux, M.-C.; Abou-Gamra, Z. *Inorg. Chim. Acta* **1986**, *118*, 115−118. (c) Dürr, H.; Hayo, R.; David, E.; Willner, I.; Zahavy, E. *Rec. Trav. Chim. Pays-Bas* **1995**, *114* (11−12), 549−555. (d) Darwent, J. R.; Douglas, P.; Harriman, A.; Porter, G. and Richoux, M.-C. *Coord. Chem. Rev.* **1982**, *44*, 83−126.

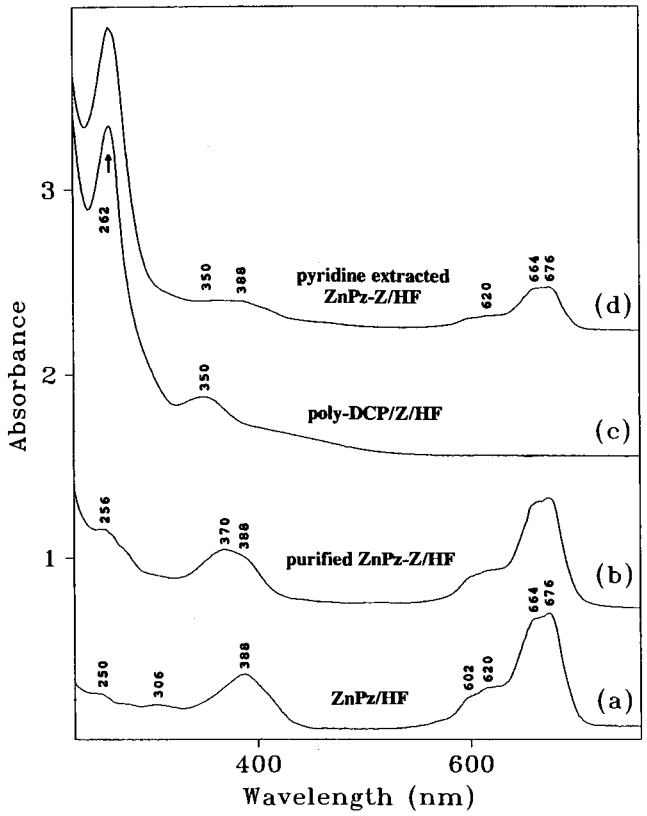

Figure 3. UV−visible spectra acquired for (a) HF extract of ZnPz; (b) HF extract of ZnPz-Z (1:15) after purification with boiling 20% NaCl; (c) HF extract of products of DCP noncyclic condensation obtained from NH_4^+-Z/DCP upon heating at 200−210 °C; (d) HF extract of ZnPz-Z (1:15) before purification with boiling 20% NaCl. All spectra were acquired after pH adjustment to 4 and centrifugation of the resulting solution.

cations is insufficient (below the required level). Accordingly, when Zn^{2+}-Z was replaced by NH_4^+-Z, only poly-DCP was generated (for the preparation of NH_4^+-Z see Experimental Section). The UV−visible spectrum of the HF extract of the NH_4^+-Z/DCP product exhibits bands at 262 and 350 nm with a shoulder at 420 nm, as shown in Figure 3c, whereas its emission spectrum shows luminescence centered at 520 nm, as shown in Figure 4.

To determine the purity of the "pyridine-extracted ZnPz-Z" samples, the zeolitic matrix was destroyed with 3% HF and the resulting solution, after pH adjustment to 4, was examined by UV−visible and emission spectroscopies, see Figures 3d and 4 (dotted line). As expected, this HF extract contained protonated forms of ZnPz complex. However, poly-DCP species were also found. This indicates that the pyridine extraction of the crude ZnPz-Z was not able to remove all impurities. Therefore, the emission spectrum of the "pyridine extracted ZnPz-Z" (1:15) in Figure 5 (dotted line) exhibits two bands centered at λ_{em} = 500 and 705 nm. The relative intensity of the high-energy emission band is 4−5 times larger than that centered at λ_{em} = 705 nm. Because the absorption of ZnPz complex appears at λ_{max} = 676 nm, [13] the luminescence centered at 500 cannot be assigned to fluorescence of the ZnPz-Z complex. However, it can be related to poly-DCP. On the other hand, the emission at λ_{em} = 705 nm can be assigned to fluorescence of the intrazeolitic ZnPz, given its similarity to that of the free ZnPz complex (λ_{em} = 683 nm),[13b,c] and the fact that fluorescence of Z/ZnPz complex adsorbed onto the outer surface of the zeolite appears at λ_{em} = 681 nm (the preparation of Z/ZnPz is presented in Experimental Section). These spectroscopic data provide

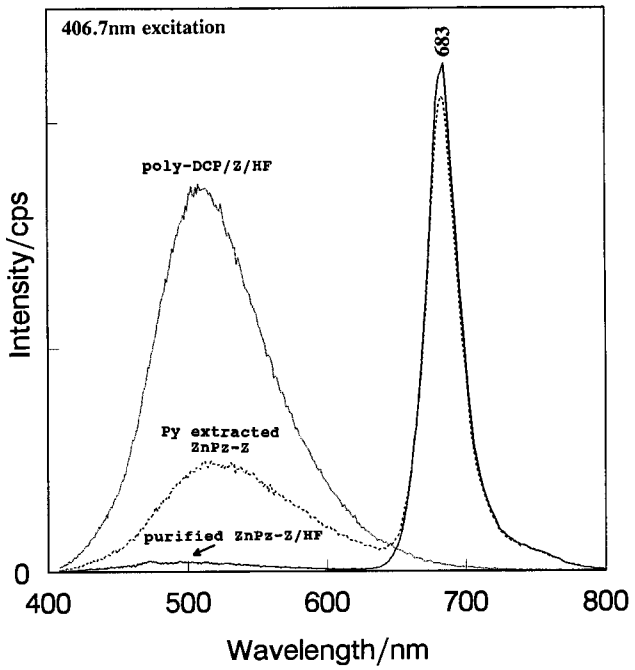

Figure 4. Emission spectra (λ_{ex} = 406.7 nm, 23 °C) acquired for (solid line) HF extract of ZnPz-Z (1:15) after purification with boiling 20% NaCl; (thin line) HF extract of poly-DCP generated during heating of NH_4^+-Z/DCP at 200−210 °C; (dotted line) HF extract of ZnPz-Z (1:15) before purification with boiling 20% NaCl.

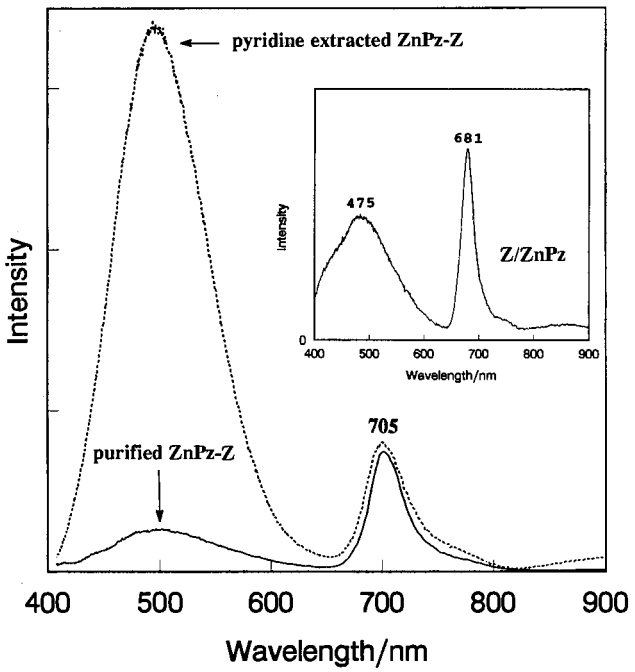

Figure 5. Emission spectra (λ_{ex} = 406.7 nm, 23 °C) acquired for: (dashed line) pyridine-extracted ZnPz-Z (crude ZnPz-Z with load of 1:15 after Soxhlet extraction with pyridine for 6 weeks; acetone for 7 days; and ethanol for 7 days); (solid line) the same sample of ZnPz-Z but after purification with boiling 20% NaCl, purified ZnPz-Z. The insert shows emission spectrum of Z/ZnPz (λ_{ex} = 351 nm, 23 °C).

evidence that the pyridine-extracted ZnPz-Z samples did not contain surface-adsorbed ZnPz; however, they were contaminated with poly-DCP species.

It is important to note that the emission spectrum of Z/ZnPz, beside the band at λ_{em} = 681 nm, also exhibits luminescence at 475 nm, as shown in the insert of Figure 5. The high-energy band at 457 nm apparently comes from those impurities (poly-

DCP) known to contaminate the ZnPz sample as indicated in the Experimental Section. Inasmuch as the poly-DCP could not be removed by pyridine extraction, it clearly has a stronger affinity for zeolite than ZnPz. Thus, in the preparation of the Z/ZnPz, those luminescent impurities are concentrated.

For further purification of the pyridine extracted ZnPz-Z samples, they were treated with hot aqueous NaCl (20% NaCl is commonly used for removing of all ionic species adsorbed onto zeolites).[9] For this, the ZnPz-Z zeolites were suspended in boiling 20% aqueous NaCl and stirred for 1 h. Subsequently, they were filtered, and then the emission and absorption spectra of the filtrate acquired. The emission spectrum of the NaCl filtrate, with 350.9 nm excitation, exhibits luminescence at λ_{em} = 500 nm, a value which closely matched that observed for the pyridine-extracted ZnPz-Z samples. In addition, the absorption spectrum of the NaCl filtrate shows absorption centered at λ_{max} = 264 nm, with a shoulder at 405 nm. The 264 nm absorption band closely matches that found for the HF extract of the pyridine extracted ZnPz-Z zeolite. Thus, the ZnPz-Z samples were washed several times with boiling NaCl (3 × 500 mL) until the NaCl filtrate did not show any absorption at 264 nm.

The UV−visible spectrum of the resulting (purified) ZnPz-Z (with the load of 1:15) HF extract matches quite well that obtained for the authentic ZnPz, although a small background increase in the wavelength range between 200 and 300 nm and an extra band at 370 nm is noted, see Figure 3a and b. Moreover, the emission spectrum of this HF extract (see Figure 4, solid line), exhibits the strong band at λ_{em} = 683 nm due to fluorescence of the free ZnPz complex and only a very weak band near 500 nm. For comparison, the emission spectrum of the solid ZnPz-Z sample (1:15) after the purification with 20% NaCl shows an obvious decrease of the band at 500 nm (ascribable to poly-DCP) by 14-fold compared to that of the pyridine-extracted ZnPz-Z (see Figure 5). These data indicate that the final ZnPz-Z sample was only slightly contaminated by the species emitting at 500 nm. Unfortunately, the emission spectrum acquired for this zeolite did not change even though it was washed or stirred in boiling 20% NaCl for days. This may suggest that the remaining impurities are entrapped within the zeolite supercages. Possibly, the DCP noncyclic condensation resulted in generation of intrazeolitic and extrazeolitc impurities (trimers or larger oligomers), but only the extrazeolitc species can be washed out using boiling 20% NaCl. The GC−MS analysis performed for the NaCl filtrate exhibits compounds with molecular ion peaks at *m*/*z* 438 and 458 which correspond well to that of hydroxylated $[DPC]^{\bullet}_3$ trimer.

To attempt to remove the intrazeolitic impurities two other purification methods were undertaken. In the first approach, the ZnPz-Z sample was treated with O_2 at 150 °C for 24 h, followed by washing with boiling 20% aqueous NaCl and then with DI water. In the second method, the ZnPz-Z zeolite was treated with boiling 3% H_2O_2 for 1 h, and then filtered. It was considered possible that the impurities might be selectively oxidized to water soluble forms. Unfortunately, as evidenced by emission spectroscopy, the ratio of the emission band at λ_{em} = 705 nm to that at λ_{em}= 500 nm decreased upon the treatments, indicating partial decomposition of the target species, ZnPz-Z.

Structural Characterization of ZnPz and Z-ZnPz Using Em, RR, and DR Spectroscopy. The UV−visible spectrum of the metal-free porphyrazine Pz (5×10^{-6} M) in pyridine consists of a number of broad bands assigned, in a manner analogous to that of porphyrin and phthalocyanine systems,[11b,14] to two $\pi(a_{1u}, a_{2u}) \rightarrow \pi^*(e_g)$ transitions, a B or Soret band at

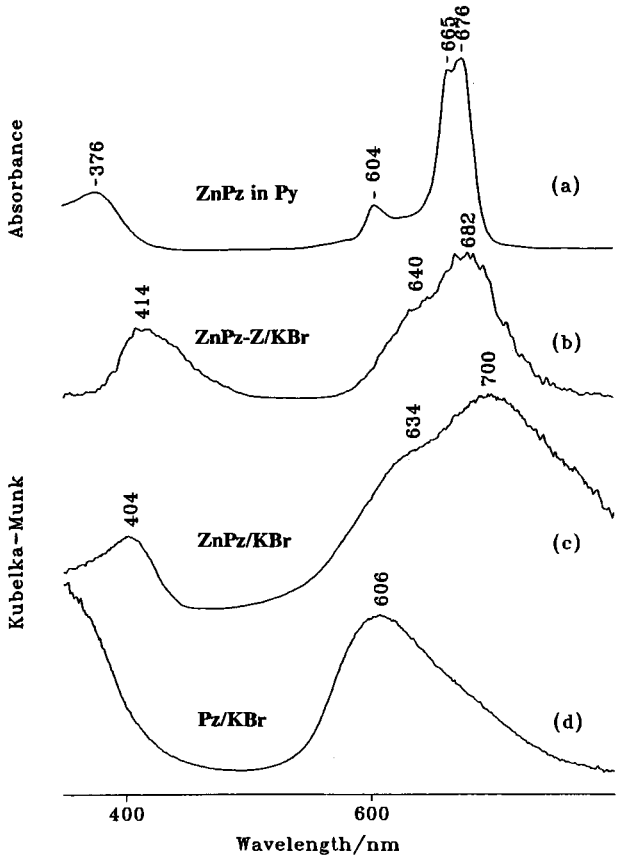

Figure 6. (a) UV−visible spectrum of ZnPz in pyridine (10^{-5} M), (b) diffuse reflectance spectrum of ZnPz-Z (1:15) in solid KBr, ZnPz-Z/KBr (0.5 mg/2 g KBr); (c) diffuse reflectance spectrum of ZnPz in solid KBr, ZnPz/KBr (0.05 mg/2 g KBr); (d) diffuse reflectance spectrum of Pz in solid KBr, Pz/KBr (0.05 mg/2 g KBr).

λ_{max} = 350 nm and a Q-band in the red region (see the diagram in Figure 2). As shown in Figure 2 (dotted line), the Q-band is split into four vibronic components with peak positions at λ_{max} = 604, 630, 660 and 688 nm. By analogy with the known metal-free phthalocyanine (Pc) spectroscopic assignment,[11b,14] the last two low-energy vibrational bands come from the Q_y-(0,0) and Q_x (0,0) zero-phonon electronic transitions, and the bands at λ_{max} = 604 and 630 are due to the $Q_y(0,1)$ and $Q_x(0,1)$ transitions, respectively. For a more concentrated solution, significant spectroscopic changes, associated with Pz dimerization, were found. For a 0.1 N HCl solution, the Pz dimers show only two electronic transitions at λ_{max} = 304 and 582 nm which correspond well to those assigned to the $[Pc]_2$ counterpart.[11b]

For the dilute ZnPz complex (10^{-5} M) in pyridine, the Q vibronic bands are less resolved compared to those of the Pz metal-free porphyrazine. They are localized at λ_{max} = 604, 630, 665, and 676 nm, as shown in Figure 6a. The appearance of the four vibrational bands suggests that the ZnPz sample contained mainly the isomer which belongs to the D_{2h} point group.[13a] In contrast, the ZnPc phthalocyanine complex has D_{4h} symmetry, [14] thus its electronic spectrum shows only two Q vibrational bands at λ_{max} = 672 and 606 nm assigned to the Q(0,0) and Q(0,1) transitions, respectively.[11b,14]

In Figure 6c and d are presented the diffuse reflectance (DR) spectra of the ZnPz complex and the free porphyrazine (Pz), thoroughly ground and pressed in solid KBr. Referring to the

(14) (a) Seybold, P. G.; Gouterman, M. *J. Mol. Spectrosc*. **1969**, *31*, 1−13. (b) Edwards, L.; Gouterman, *J. Mol. Spectrosc*. **1970**, *33*, 292−310.

UV−visible spectrum of concentrated Pz in 0.1 N HCl, the broad reflectance band observed for the Pz/KBr at $\lambda_{max} = 606$ nm can be assigned to the $[Pz]_2$ dimers. However, the sideband occurring to the red, at 685 nm, indicates the presence of a small amount of the monomeric Pz species.

In the spectra of solid samples illustrated in Figure 6 the Q-bands are much broader and red shifted with respect to those observed for the ZnPz complex in pyridine solution. In the case of ZnPz in KBr the broadening can be explained by possibly large contribution of ZnPz regular (specular) reflectance which can occur for highly absorbing materials.[12] In addition, the size of ZnPz clusters may vary and give rise to broadening. The DR bands of the ZnPz-Z samples (Figure 6b) are also broader and red shifted with respect to those of ZnPz diluted in pyridine (6 nm for Q-band and 36 nm for B band), though, their width is smaller than that of ZnPz in KBr. We note that broadening of the intrazeolitic ZnPz complex DR bands generally did not change with the ZnPz-Z load (the wavelength and size of the DR bands for the samples with loads of 1:5 and 1:15 are identical) and cannot be attributed to specular reflectance contributions. This slight broadening for the ZnPz-Z samples is more reasonably attributed to site heterogeneity in the zeolite as has been noted for other zeolite-entrapped complexes.[8]

Emission spectra of the purified ZnPz-Z were acquired using excitation lines at $\lambda_{ex} = 350.9$, 406.7, and 647.1 nm. As has been discussed above, the very weak high-energy band centered at $\lambda_{em} = 500$ nm in Figure 5 is attributable to impurities. However, the strong band at 705 nm is assigned to fluorescence of the ZnPz complex entrapped within the zeolite. In pyridine solution, the ZnPz complex and the metal-free Pz porphyrazine exhibit fluorescence at $\lambda_{em} = 683$ and 696 nm, respectively, which correspond well to that of ZnPc and Pc analogues.[13,15] Thus, the emission maximum for ZnPz-Z is 22 nm (457 cm^{-1}) red shifted with respect to that of the ZnPz complex dissolved in pyridine. It is important to recall that the diffuse reflectance bands of the ZnPz-Z/KBr sample also exhibited a 6 nm (130 cm^{-1}) red shift for the Q-band and a 36 nm (2300 cm^{-1}) red shift for the B band with respect to those of the ZnPz complex in pyridine solution, as illustrated in Figure 6.

In an attempt to acquire more detailed structural information on the intrazeolitic ZnPz, resonance Raman (RR) spectroscopic studies were performed. The Raman spectra of the ZnPz/KBr, the Pz/KBr, and the purified ZnPz-Z samples, obtained with 568.2 nm excitation, are shown in Figure 7. First, it is important to note that there are distinct differences in the spectra of the ZnPz and free Pz samples (traces a and b), which are useful in documenting any possible contamination of the ZnPz-Z sample with free Pz. Thus, free Pz exhibits distinct features at 1545, 1090, 808, and 724 cm^{-1} which are not coincident with modes of ZnPz. The absence of these features in the RR spectrum of the purified ZnPz-Z sample (trace c) confirms the fact that the ZnPz-Z sample obtained here does not contain any free Pz.

It has been recently demonstrated[5a,b] that the influence of the Y-zeolite framework on the ground-state structure of polypyridine Ru^{2+} complexes is minor. However, small frequency shifts (a few wavenumbers) were observed for some bands.[5] Inasmuch as these larger ZnPz complexes are expected to be more susceptible to distortion by the supercages than the smaller polypyridine complexes, it is important to acquire the RR spectra of these ZnPz-Z samples. Significant spectroscopic changes are expected if the generation of intrazeolitic ZnPz results in a structural distortion of the ZnPz complex accompanied by symmetry lowering.

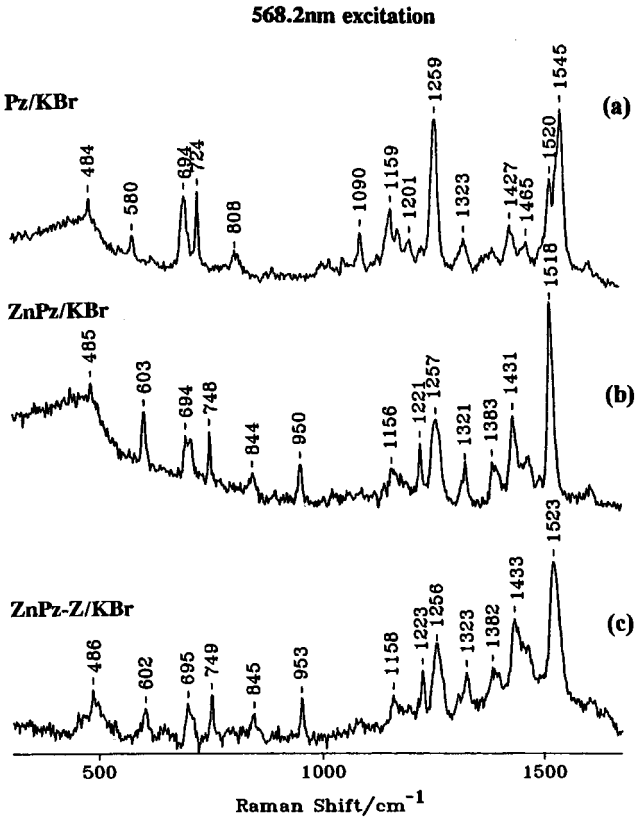

Figure 7. Raman spectra ($\lambda_{ex} = 568.2$ nm, 23 °C) acquired for (a) Pz in solid KBr (Pz/KBr), accumulation of 4 scans; (b) ZnPz in solid KBr (ZnPz/KBr), accumulation of 4 scans; (c) ZnPz-Z (1:15) in solid KBr (ZnPz-Z), accumulation of 16 scans.

As can be clearly seen by comparing the RR spectra shown in traces b and c of Figure 7, entrapment of ZnPz within the supercages of Y-zeolite does not induce large shifts in any of the structure sensitive vibrational modes, the largest shift observed being 5 cm^{-1} for the feature located near 1520 cm^{-1}. This band is reasonably attributable to symmetric C−C and C−N stretching modes involving mostly pyrrole and azomethine groups in the ZnPz macrocycle, by comparison to the vibrational assignments performed for ZnPc analogue[16a,b] and the free porphyrazine.[16c] Thus, based on these RR data, the ZnPz molecule can apparently reside within the (∼13 Å diameter) supercage without experiencing substantial distortion. Presumably, out-of-plane deformations of the ZnPz macrocycle required to allow the peripheral pyridine rings to protrude through the tetrahedrally arranged windows are relatively small and induce only 1−5 cm^{-1} frequency blue shifts in some vibrational modes.

Concluding Remarks

The condensation of 3,4-dicyanopyridine (DCP) around the intrazeolitic Zn^{2+} cations results in production of the zeolite-entrapped ZnPz complex. Because this reaction requires a large excess of DCP (4 DCP per supercage), the generation of ZnPz-Z is accompanied with production of the metal-free porphyrazine

(15) Assour, J. M.; Harrison, S. E. *J. Am. Chem. Soc*. **1965**, *87*, 651−652.

(16) (a) Palys, B. J.; van den Ham, D. M. W.; Briels, W.; Feil, D. *J. Raman Spectrosc*. **1995**, *26*, 63−75. (b) Melendres, C. A.; Maroni, V. A. *J. Raman Spectrosc*. **1984**, *15*, 319−326. (c) Braun, D.; Ceulemans, A. *J. Phys. Chem*. **1995**, *99*, 11101−11114.

and DCP noncyclic oligomers. The latter species are, presumably, terminated by side-reactions with O_2 or H_2O.

Spectroscopic characterization of the zeolite-entrapped ZnPz indicate that the ground state structure is apparently quite similar to that of the free complex. Thus, the frequencies of the vibrational modes of the ZnPz-Z are virtually identical to those of the free complex, whereas it is known that nonplanar distortion of large macrocycles, such as metalloporphyrins, can cause substantial shifts in certain structure-sensitive modes.[17] This observation is in conflict with calculations which predict significant nonplanar distortions for zeolite-entrapped metallophthalocyanines, a structural analogue of ZnPz.[2c,7a] The most dramatic spectroscopic consequence of entrapment is an observed 22 nm red shift in the emission maximum (i.e., 683 vs 705 nm), a shift which presumably arises because of interactions with the zeolite framework which stabilize the excited state.

Acknowledgment. This work was supported by a grant from the Division of Chemical Science, U.S. Department of Energy (Grant DE-FG-02-86ER13619).

IC971118S

(17) (a) Anderson, K. K.; Hobbs, J. D.; Luo, L.; Stanley, K. D.; Quirke, J. M. E.; Shelnutt, J. A. *J. Am. Chem. Soc.* **1993**, *115*, 12346−12352. (b) Alden, R. G.; Crawford, B. A.; Doolen, R.; Ondrias, M. R.; Shelnutt, J. A. *J. Am. Chem. Soc.* **1989**, *111*, 2070−2072. (c) Song, X.-Z.; Jentzen, W.; Jia, S.-L.; Jaquinod, L.; Nurco, D. J.; Medforth, C. J.; Smith, K. M.; Shelnutt, J. A. *J. Am. Chem. Soc.* **1996**, *118*, 12975−12988. (d) Shelnutt, J. A.; Song, X.-Z.; Ma, J.-G.; Jia, S.-L.; Jentzen, W.; Medforth, C. J. *Chem. Soc. Rev.* **1998**, *27*, 31−41.